The Empirical Delay Time Distributions of Type Ia Supernovae From Galaxy Star Formation Histories

L.-G. Strolger, Pacifici, Rodney, et al.

ABSTRACT

blah, blah, blah . . .

1. Introduction

There have been several measures of the volumetric SN Ia rate at various redshifts by various groups. These rate values have not always been in total agreement with one another, and there may be several valid reasons as to why (see rev. by Haden?). But as there is little concession on which is the most appropriate way to express measures in event rates, it it probably best to consider each as a valid measure. Further, we assume each is valid within their measured statistical error, which again may be bold, but is probably satisfactory given the number of rate measures in each redshift interval.

It would be reasonable to assume the volumetric rates follow a broken power law evolution with redshift, i.e., $R_{Ia} = R_0 (1 + z)^A$ where at $z < 1$ the power-law slope is $A = 1.50 \pm 0.02$ (with $R_0 = 2.5 \pm 0.2 \times 10^{-5}$ yr^{-1} Mpc^{-3} h_{70}^3), which flattens substantially to $A = -0.03 \pm 0.2$ at redshifts greater than 1 (see Figure 1).

For these types of analyses, the standard assumption is that the stellar death rate (or supernova rate) is related to the stellar birth rate, convolved with some delay-time distribution that contains all the temporal factors of stellar evolution (e.g., main sequence lifetime, etc.) and binary star evolution (e.g., accretion rates or merger times). Two additional terms include the fraction of the initial mass function (or IMF) that are the progenitors to the SNe Ia (presumably $3 - 8 \, \mathrm{M}_\odot$ zero-age main sequence stars), and the fraction of that population that are actually capable of producing events, as not are necessarily in the right type of binary system or systems.
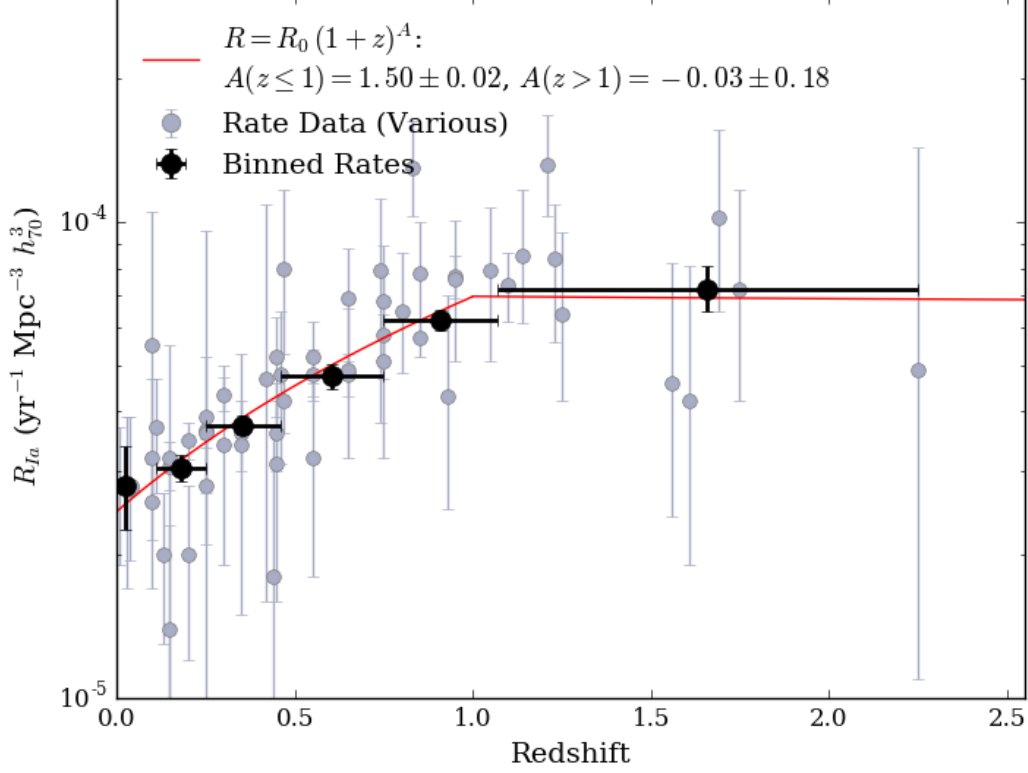
Fig. 1.— Type Ia supernova volumetric rate measures from various sources in the literature (gray points, also see Table), and binned (black points) for illustration. Red lines show a broken power-law fit to the data in redshift space.

We can relate volumetric SN Ia rate history to the cosmic star formation history($\dot{\rho}_\star$) in a similar way, expressed mathematically by,

$$R_{\mathrm{Ia}}(t) = k\,\varepsilon\left[\dot{\rho}_\star(t) * \Phi(t)\right], \tag{1}$$

where $\Phi(t)$ is the delay-time distribution of SNe Ia, k is the fraction of the IMF (by mass) responsible for SN Ia progenitors, ε is the fraction of that population that are ultimately successful in producing SNe Ia, and t is the forward-moving clock of the universe.

1.1. The fraction of stars responsible for SNe Ia

Dissecting each of these terms, k is perhaps the easiest to approximate. The progenitors of SNe Ia have traditionally been CO WD which acquire sufficient mass to approach or exceed the Chandrasekhar mass limit, $M_{ch} = 1.44\,M_{\odot}$. To only marginally achieve this, they can either start at sufficiently high mass to require only a small amount of accretion from a nearby companion (typically single-degenerate, or SD, scenarios), or as a pair of WD that have a combined mass that meets this criterion (the double-degenerate, or DD, scenario) setting an even lower constraint (see Maoz et al. 2013, for a review). In the case of WD/WD mergers, WD mass distributions are strongly peaked around $M_{WD} \approx 0.6 \pm 0.1\,M_{\odot}$ (Catalán et al. 2008), in which a pair drawn from such distribution may be satisfactorily close to the ignition threshold of a carbon core for a nonrotating CO WD, approximately $1.38\,M_{\odot}$ of Arnett (1969) and Nomoto (1982). Initial-Final Mass relations (e.g., Catalán et al. 2008; Cummings et al. 2018) would correspond these to ZAMS masses of approximately $3\,M_{\odot}$, but no less than $\sim 2.5\,M_{\odot}$.

The same Initial-Final Mass relations would suggest that WD essentially at M_{ch} would fall just below $8\,M_{\odot}$ ZAMS. On a more physical bases, simulations show that the lowest mass in which C ignition is still possible is around $6-8\,M_{\odot}$ Chen et al. (2014); Denissenkov et al. (2015), but likely no more than $\sim 11\,M_{\odot}$ (Takahashi et al. 2013), above which an electron-capture-induced collapse mechanism begins, marking the onset of core-collapse supernovae.

It is reasonable, therefore, to assume a progenitor mass range of about $3-8\,M_{\odot}$ ZAMS. From a numerical assessment of these stars, assuming they fall within an IMF that is a power-law distribution by mass (in this initial mass range) with $\alpha \approx -2.3$ (Salpeter 1955;

Kroupa 2001), one would expect

$$k = \frac{\int\limits_{3M_\odot}^{8M_\odot} \xi(M)\,dM}{\int\limits_{0.1M_\odot}^{125M_\odot} M\,\xi(M)\,dM}, \tag{2}$$

where $k = 0.021^{+33\%}_{-24\%}\,M_\odot^{-1}$. The error in k is driven more by choices in the upper and lower value in the selected mass range of SN Ia progenitors than by the choice in IMF model, as described above.

The fraction of CO WDs that are successful in making SNe Ia is hard to determine, as we don't quite yet know the details of the progenitor mechanism or mechanisms. Estimates swing rather wildly from (perhaps) from as low as 1 in 200 (Breedt et al. 2017) to as optimistic as 1 in 40 (Maoz & Mannucci 2012). There is at least strong consensus that accretion on to a CO WD is essential, but very different plausible WD close binary scenarios from at least a theoretical standpoint (Nelemans et al. 2001a,b). The binary fractions of WDs has been recently estimated from the the ESO-VLT Supernova-Ia Progenitor Survey (Napiwotzki et al. 2007, SPY) show close double WD systems may have $\varepsilon_{\rm bin} \simeq 0.1 \pm 20\%$, with separations distributed following a power-law slope of $\alpha = -1.3 \pm 15\%$ (Maoz & Hallakoun 2017). It is not likely all of these successfully yield SNe Ia as their merger rates in the MW are at least a magnitude higher than best estimates of the SN Ia rate in our galaxy, and presumably some of these will form AM CVn and R Corona Borealis stars, but at least it could be treated as an upper limit on ε.

1.2. The star-formation density history

The cosmic star formation history (CSFH), at least to $z < 5$, or over 90% of the history of the universe, is fairly well understood, with Madau & Dickinson (2014) providing one of the most complete compilations. However there is significant scatter in individual

tracers of the compilation, as some are provided from limited probed volumes leading to large uncertainties in fluctuations with cosmic variance. The CSFH data derived recently from the combined GAMA, G10-COSMOS, and 3D-HST datasets by Driver et al. (2018) is alternatively done in a quasi-homogeneous analysis over a larger area, leading to greatly reduced total uncertainties. The derived trend is somewhat consistent with Madau & Dickinson (2014), but has a notably weaker peak at 'cosmic noon' ($z \sim 2$) and a slower build-up of unobscured star-formation at high-z (see Figure 2). Using the parameterization in Madau & Dickinson (2014), where

$$\dot{\rho}_\star(z) = \frac{A\,(1+z)^C}{((1+z)/B)^D + 1}.$$ (3)

We fit the above function to MD14 data using a Levenberg-Marquardt least-squares algorithm, resulting in the solid blue line and error region shown in Figure 2, with $A = 0.013 \pm 0.001$, $B = 2.6 \pm 0.1$, $C = 3.2 \pm 0.2$, and $D = 6.1 \pm 0.2$, slightly different from the values fit in MD14. The same functional fit to the Driver et al. (2018) data yields $A = 0.009 \pm 0.001$, $B = 2.7 \pm 0.5$, $C = 2.5 \pm 0.4$, and $D = 4.1 \pm 0.3$.

[NOTE: more on which is the better choice, or if analysis on the end should be done on both.]

1.3.   SN Ia progenitor delay times

[NOTE: talk about the expected delay-time distribution, values from Graur and Maoz, inability to probe turnover at 'SN high noon', around $z \sim 1$.]

Following Strolger et al. (2010), we can continue to test a robust delay-time model, capable of reproducing the theoretical distributions for SD and DD models at one extreme, and δ-function delay times at the other. The unimodal, skew-normal $\Phi(\tau)$ function is defined as:
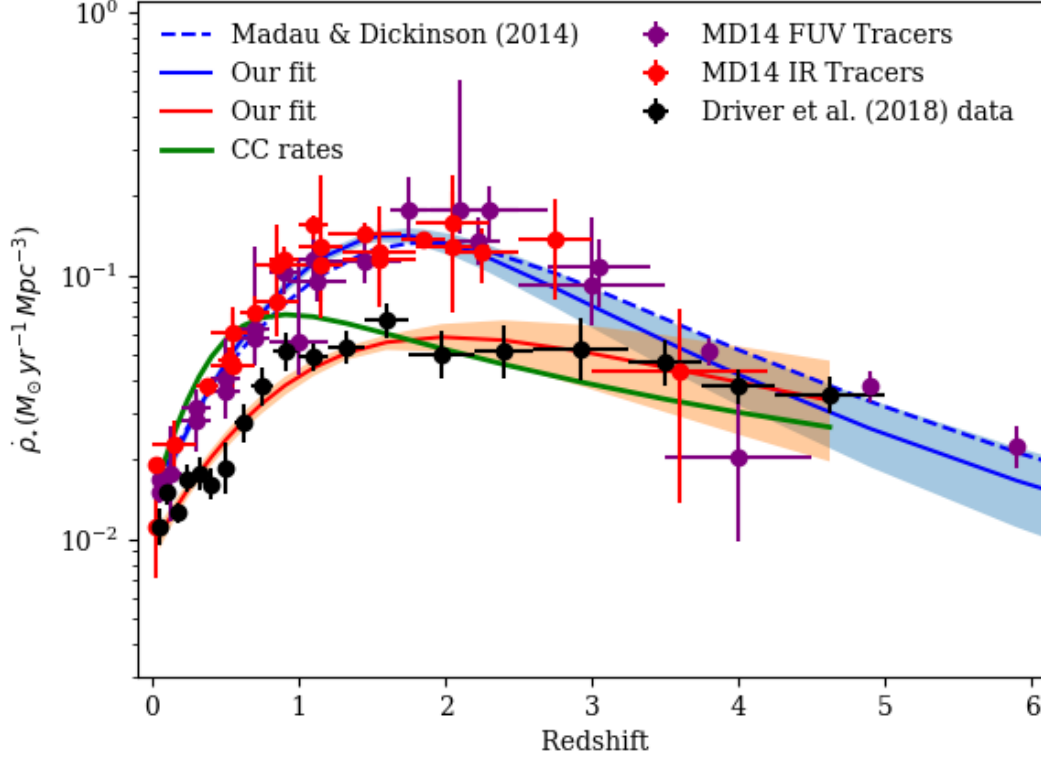
Fig. 2.— Shown are the compendium cosmic star formation histories, from Madau & Dickinson (2014) and Driver et al. (2018). Lines are fits to the data as indicated, and shaded regions represent the 1-σ confidence intervals to the fits. Also shown for comparison is the model fit to core-collapse SN rates from Strolger et al. (2015).

$$\Phi(\tau) = \frac{1}{\omega\pi} \exp\left(\frac{-(\tau - \xi)^2}{2\omega^2}\right) \int_{-\infty}^{\alpha\left(\frac{\tau-\xi}{\omega}\right)} \exp\left(\frac{-t'^2}{2}\right) dt', \tag{4}$$

where location (ξ),[1] width (ω^2), and shape (α) define the mode time $(\bar{\tau})$, variance (σ^2), skewness (γ_1), and kurtosis (γ_2) of the model function by,

---

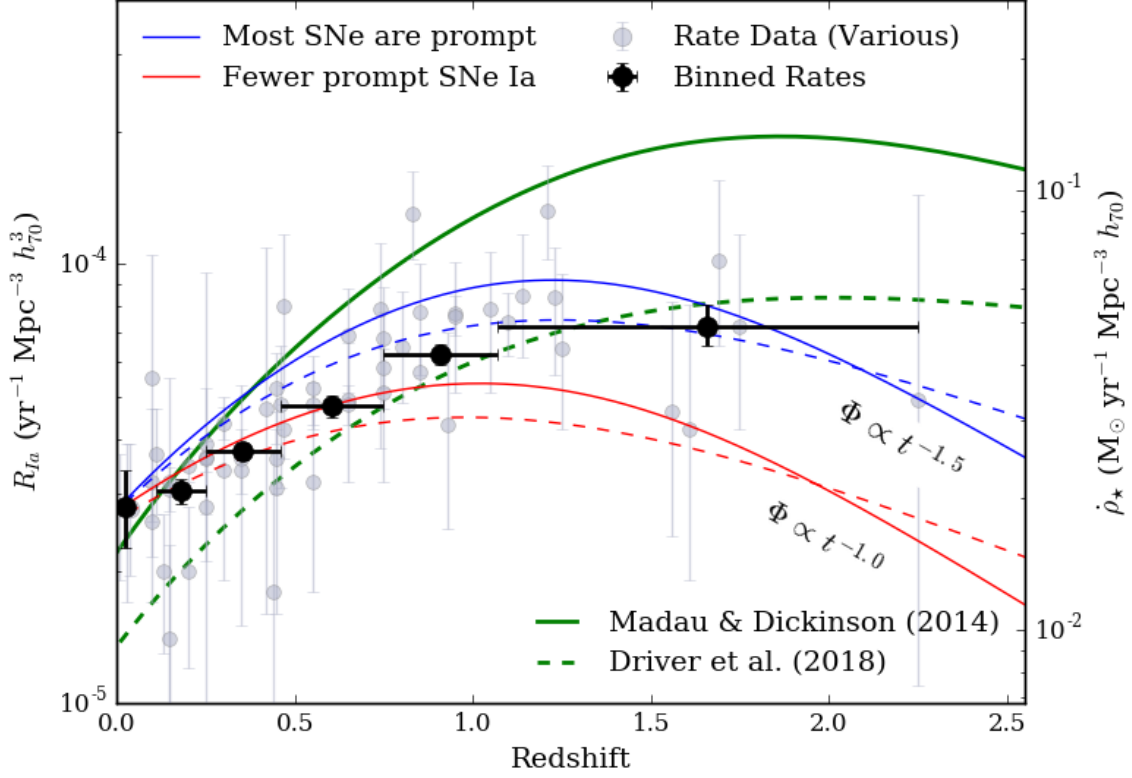[1]Different from the initial mass function, $\xi(M)$.

Fig. 3.— Shown in comparison to the data are the expected volumetric rates for power-law delay-time distributions ($\alpha = 1.0$ and 1.5 in red and blue, respectively) as applied to the cosmic star formation rates (Madau & Dickinson 2014; Driver et al. 2018, in solid and dashed green, respectively). Dashed rate models require a higher fraction of WD progenitors than the solid lines.

$$\bar{\tau} = \xi + \omega\delta\sqrt{\frac{2}{\pi}},$$

$$\sigma^2 = \omega^2\left(1 - \frac{2\delta^2}{\pi}\right),$$

$$\gamma_1 = \frac{1}{2}(4 - \pi)\frac{(\delta\sqrt{2/\pi})^3}{(1 - 2\delta^2/\pi)^{3/2}},$$

$$\gamma_2 = 2(\pi - 3)\frac{(\delta\sqrt{2/\pi})^4}{(1 - 2\delta^2/\pi)^2}.$$
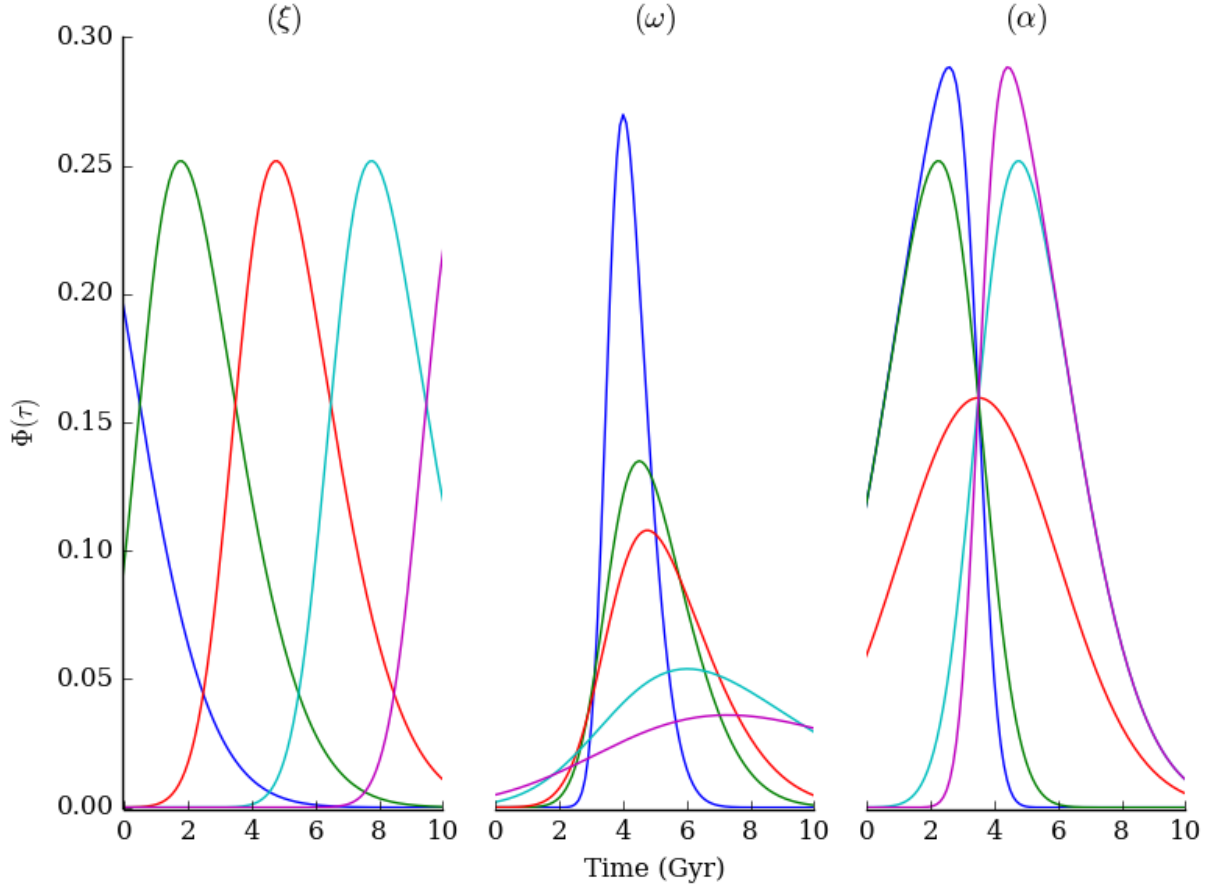
Fig. 4.— Families of delay-time distributions models shown for various values of location (ξ) fixing other parameters (left plot of figure), width (ω, middle plot), and shape (α, right plot), for illustration purposes.

where $\delta = \alpha\,(1+\alpha^2)^{-1/2}$. Figure 4 demonstrates the flexibility of the model in producing various distributions in τ.

2. Delay Time Distributions from Volumetric SN Ia Rates and the Cosmic Star Formation History

2.1. The optimized solution

We apply a maximum likelihood estimation method to determine the best-fit unimodal delay time model to Equation 1 using a method described in Hogg et al. (2010) and the `emcee.py` documentation (Foreman-Mackey et al. 2013). We assume, for simplicity, that the errors of all survey data are gaussian in nature, but may be underestimated by some factor (f), which may be correctly justified given we are only using the statistical error produced for each value.

As follows, we adopt the likelihood function to be:

$$\ln p(y|x, \sigma, \varepsilon, \xi, \omega, \alpha, f) = -\frac{1}{2} \sum_i \left\{ \frac{[R_{\mathrm{Ia},i} - \mathrm{model}(t_i; \varepsilon, \xi, \omega, \alpha)]^2}{s_i^2} + \ln(2\pi s_i^2) \right\}, \qquad (5)$$

where,

$$s_i^2 = \sigma_i^2 + f^2 \, \mathrm{model}(t_i; \varepsilon, \xi, \omega, \alpha)^2. \qquad (6)$$

We then find the optimal parameters which maximize this likelihood.

As for priors, we apply rather loose, arbitrary bounds on the optimization, in that we require the successful fraction of progenitors to be between zero and 1, that the width parameters can only be positive, and the that underestimation fraction can only be between zero and 1. Otherwise, the bounds are as follows for parameters ε, ξ, ω, α, and $\ln f$, respectively: [(0.,1.0),(-2000.,2000.),(0.001,100.),(-500.0,500.0),(-4.,0.)]. The results of that fit are shown in Figure 5, and in Table 1.

While the optimization results in values, and a rather interesting delay-time distribution, it is not directly possible to estimate the errors in the parameters via this maximum likelihood optimization method. A Markov chain Monte Carlo (MCMC) is better
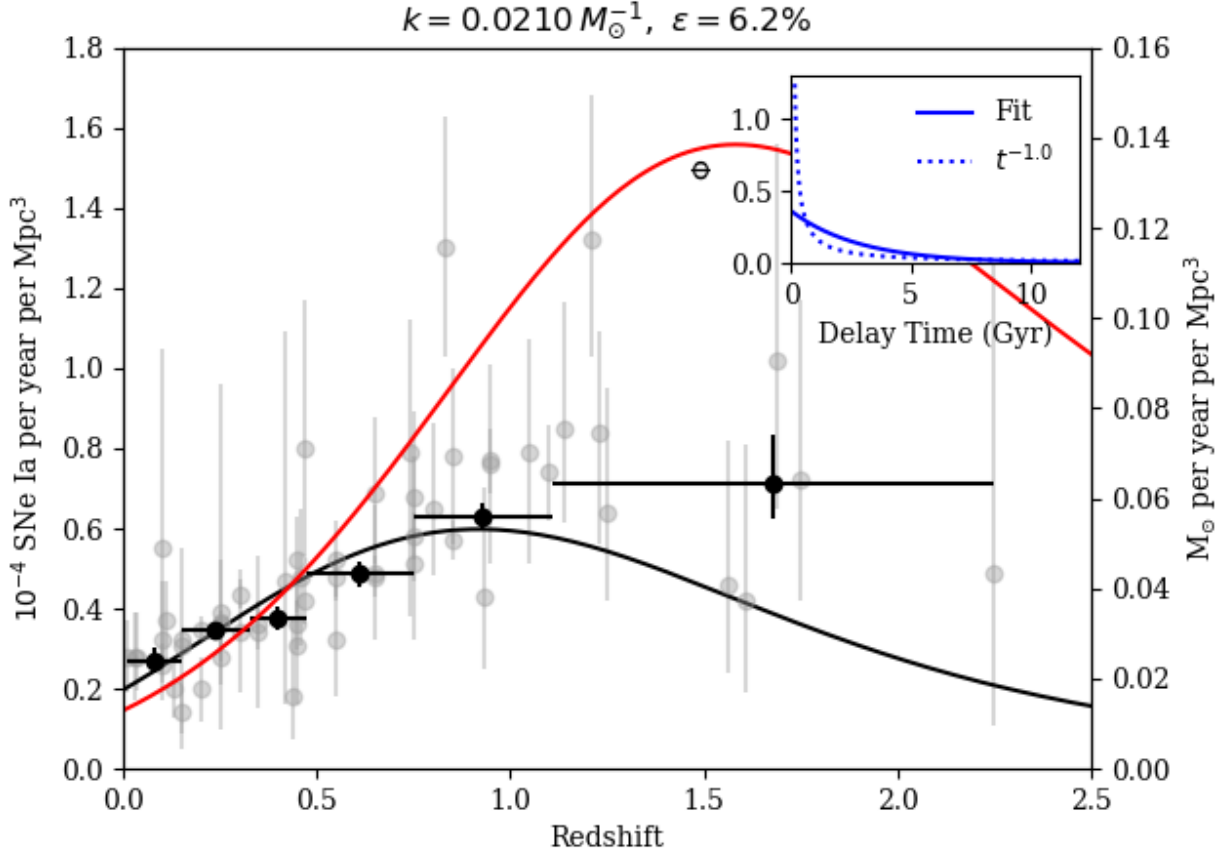
Fig. 5.— In addition to rate values shown in previous figures, the $R_{\mathrm{Ia}}(z)$ result of from optimal parameter fitting is show (black line). The CSFH is shown on in red, and along the secondary abscissa.

suited for that.

2.2. The MCMC solution

Exploring the parameter space in an MCMC allows both confirmation of the optimized solution and an exploration of the range of validity. We use the affine Invariant MCMC ensemble sampler from `emcee.py` (Foreman-Mackey et al. 2013), and use the same likelihood function as shown in Equation 5, and set our uniform priors as described by the bounds,

as shown in the previous section. We then set 1,000 walkers to explore 10,000 steps, for a total of 10 million iterations, the first 100,000 of which we discard as 'burn-in'. The results of which are shown in Figure 6 and Table 1.

As is shown, there is a clear convergence in $\ln f$, the factor by which reported errors in rate measures are underestimated. It seems that nearly all values are underestimated by less than 33%, with most only 10% underestimated. While there is a large dispersion in rate values, and seemingly inconsistent rates in some of the same redshift ranges, their statistical errors are not grossly underestimated. As fairly well constrained is ε, suggesting (as expected) only $10 \pm 10\%$ of WD stars contribute as SN Ia progenitors. That number increases to $0.14^{+0.13}_{-0.14}$ when the D18 CSFH is used. However, the parameters we wished to know the most about, ξ, ω, and α, are very much less constrained by the MCMC. There is a clear peak around $\omega \approx 60$, but that value is also highly degenerate with the value of ξ. There does not appear to be any convergence or preference in the value of α.

Table 1: Results for unimodal model

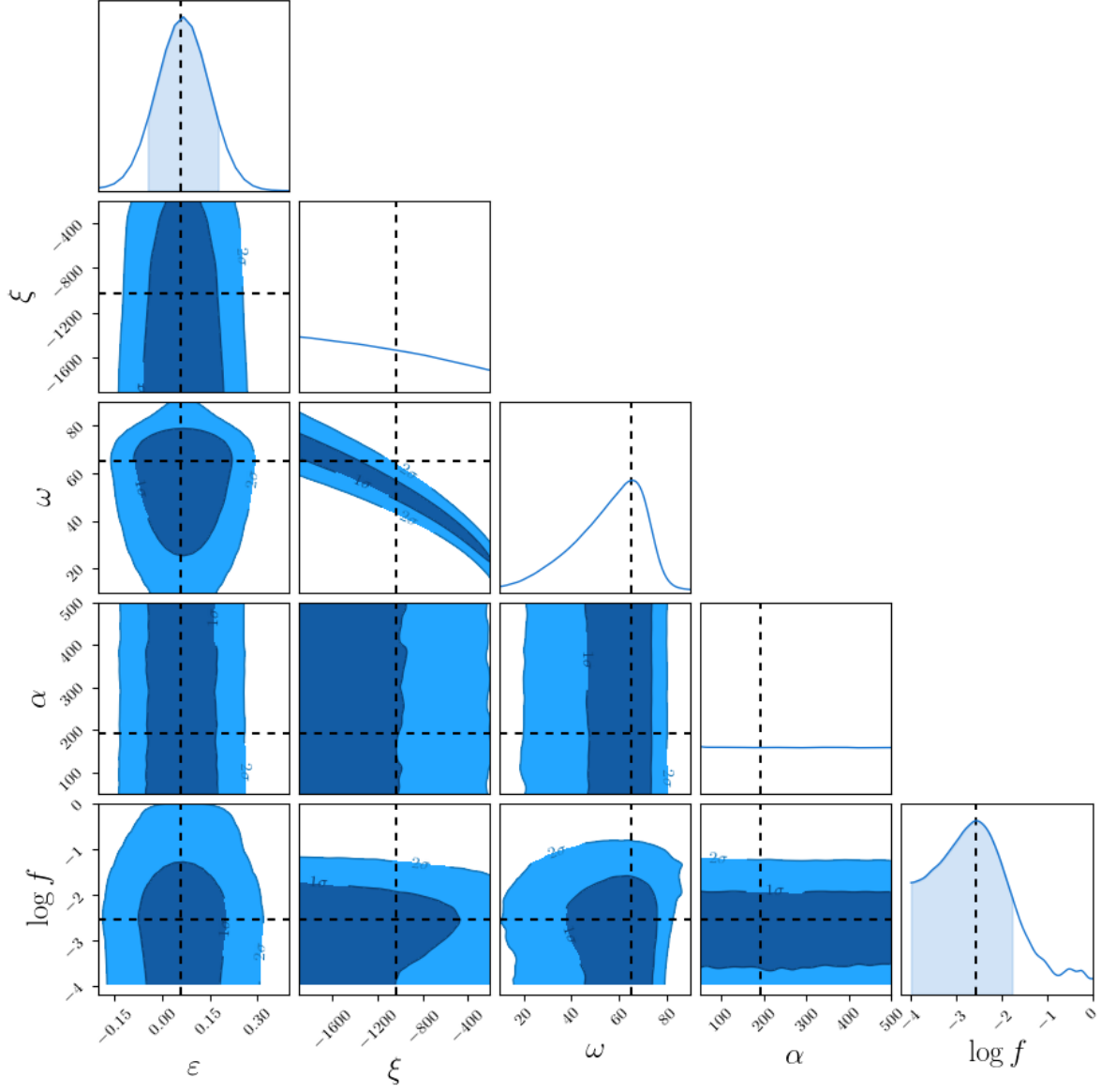| Model test	ε	ξ	ω	α	$\log f$
CSFH Max. Likelihood	0.062	-1669.7	69.1	88.7	-2.99
CSFH MCMC	0.07 ± 0.11	-1031^{+1033}_{-687}	65^{+15}_{-20}	190 ± 210	$-2.5^{+0.8}_{-1.4}$

Fig. 6.— MCMC results on unimodal delay-time distribution model, fit to volumetric rate data and CSFH. Plot generated using `ChainConsumer.py` (Hinton 2016).

3. Delay Time Distributions from Star Formation Histories

This is an evaluation of the maximum likelihood delay time distribution following the prescription of Maoz et al. (2012) but performed on the GOODS/CANDELS galaxies. In a given galaxy, the total expected rate of SNe Ia per year will be:

$$R_i = \int_0^t \Psi(t') * \Phi(\tau) \, dt' \tag{7}$$

where $\Psi(t)$ is the star formation history of the galaxy (mapped in forward time), and $\Phi(\tau)$ is the delay time distribution model, also forward in time. The product of the integrated rate and the control time, $t'_{c,i}$, which contains all the information on the temporal sampling and depth of the survey,

$$m_i = R_i \times t'_{c,i} \tag{8}$$

which is the expected number of SN Ia events from that galaxy over the duration of the survey. The probability distribution of observed events is likely Poisson, where of catching n_i SNe Ia from that galaxy when m_i are expected is

$$P(n_i|m_i) = \frac{m_i^{n_i} e^{-m_i}}{n_i!}. \tag{9}$$

The product of probabilities for all galaxies in the survey would then serve as the likelihood of a given delay-time distribution model. The log-likelihood, convenient for MCMCs, is then expressed by:cp

$$L = \prod_i^N P(n_i|M_i) \Rightarrow \ln L = -\sum^N m_i + \sum^N \ln\left(\frac{m_i^{n_i}}{n_i!}\right) \tag{10}$$

in which the last term is zero for galaxies which do not host SNe Ia during the survey.

The model parameters, ξ, ω, and α are explored in an Affine Invariant Markov-chain Monte Carlo using `emcee.py` (Foreman-Mackey et al. 2013). As for priors, we restrict the parameters to the space:
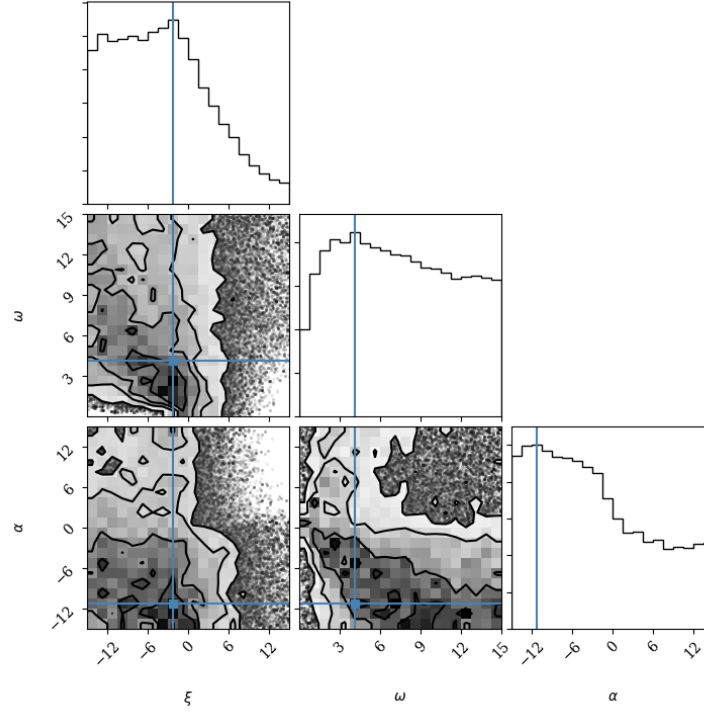
Fig. 7.— MCMC results on 147 galaxies in CANDELS, 49 of which are SN Ia hosts. Plot generated using `corner.py` (Foreman-Mackey 2016).

$$-15 < \quad \xi \quad \leq 15$$

$$0 < \quad \omega \quad \leq 15$$

$$-15 < \quad \alpha \quad \leq 15$$

4.   discusssion
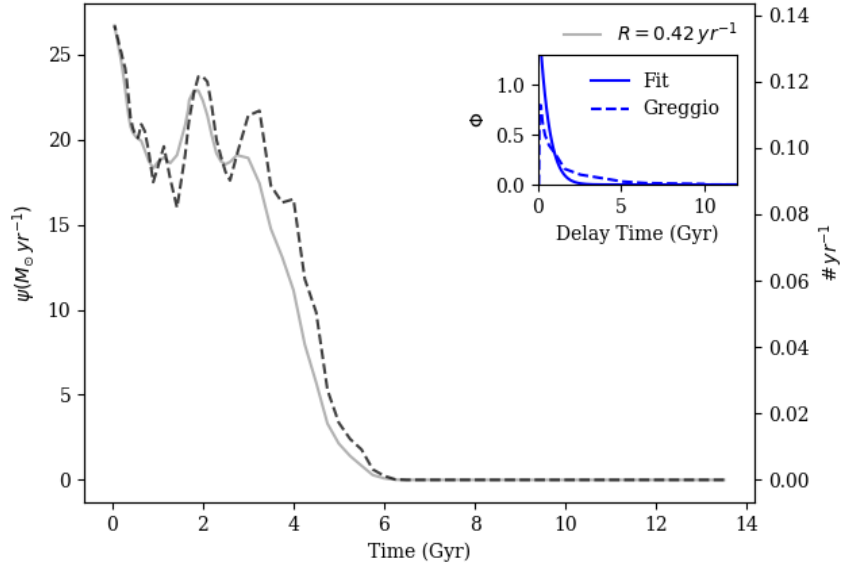
Fig. 8.— Example of best-fit delay-time distribution (inset) on the SFH of a sample host galaxy.

REFERENCES

Arnett, W. D. 1969, Ap&SS, 5, 180

Breedt, E., Steeghs, D., Marsh, T. R., Gentile Fusillo, N. P., Tremblay, P. E., Green, M., De Pasquale, S., Hermes, J. J., Gänsicke, B. T., Parsons, S. G., Bours, M. C. P., Longa-Peña, P., & Rebassa-Mansergas, A. 2017, MNRAS, 468, 2910

Catalán, S., Isern, J., García-Berro, E., & Ribas, I. 2008, MNRAS, 387, 1693

Chen, M. C., Herwig, F., Denissenkov, P. A., & Paxton, B. 2014, Monthly Notices of the Royal Astronomical Society, 440, 1274

Cummings, J. D., Kalirai, J. S., Tremblay, P.-E., Ramirez-Ruiz, E., & Choi, J. 2018, ArXiv e-prints

Denissenkov, P. A., Truran, J. W., Herwig, F., Jones, S., Paxton, B., Nomoto, K., Suzuki, T., & Toki, H. 2015, Monthly Notices of the Royal Astronomical Society, 447, 2696

Driver, S. P., Andrews, S. K., da Cunha, E., Davies, L. J., Lagos, C., Robotham, A. S. G., Vinsen, K., Wright, A. H., Alpaslan, M., Bland-Hawthorn, J., Bourne, N., Brough, S., Bremer, M. N., Cluver, M., Colless, M., Conselice, C. J., Dunne, L., Eales, S. A., Gomez, H., Holwerda, B., Hopkins, A. M., Kafle, P. R., Kelvin, L. S., Loveday, J., Liske, J., Maddox, S. J., Phillipps, S., Pimbblet, K., Rowlands, K., Sansom, A. E., Taylor, E., Wang, L., & Wilkins, S. M. 2018, MNRAS, 475, 2891

Foreman-Mackey, D. 2016, The Journal of Open Source Software, 24

Foreman-Mackey, D., Hogg, D. W., Lang, D., & Goodman, J. 2013, PASP, 125, 306

Hinton, S. R. 2016, The Journal of Open Source Software, 1, 00045

Hogg, D. W., Bovy, J., & Lang, D. 2010, ArXiv e-prints

Kroupa, P. 2001, MNRAS, 322, 231

Madau, P., & Dickinson, M. 2014, ARA&A, 52, 415

Maoz, D., & Hallakoun, N. 2017, MNRAS, 467, 1414

Maoz, D., & Mannucci, F. 2012, PASA, 29, 447

Maoz, D., Mannucci, F., & Brandt, T. D. 2012, MNRAS, 426, 3282

Maoz, D., Mannucci, F., & Nelemans, G. 2013, ArXiv e-prints

Napiwotzki, R., Karl, C. A., Nelemans, G., Yungelson, L., Christlieb, N., Drechsel, H., Heber, U., Homeier, D., Koester, D., Leibundgut, B., Marsh, T. R., Moehler, S., Renzini, A., & Reimers, D. 2007, in Astronomical Society of the Pacific Conference Series, Vol. 372, 15th European Workshop on White Dwarfs, ed. R. Napiwotzki & M. R. Burleigh, 387

Nelemans, G., Portegies Zwart, S. F., Verbunt, F., & Yungelson, L. R. 2001a, A&A, 368, 939

Nelemans, G., Yungelson, L. R., Portegies Zwart, S. F., & Verbunt, F. 2001b, A&A, 365, 491

Nomoto, K. 1982, ApJ, 253, 798

Salpeter, E. E. 1955, ApJ, 121, 161

Strolger, L., Dahlen, T., & Riess, A. G. 2010, ApJ, 713, 32

Strolger, L.-G., Dahlen, T., Rodney, S. A., Graur, O., Riess, A. G., McCully, C., Ravindranath, S., Mobasher, B., & Shahady, A. K. 2015, ApJ, 813, 93

Takahashi, K., Yoshida, T., & Umeda, H. 2013, ApJ, 771, 28

This manuscript was prepared with the AAS LATEX macros v5.2.

Table 2: Parameter Covariance MCMC SFD

	f	ξ	ω	α	$\log\phi$
f	0.41	-125.69	6.61	33.98	-0.41
ξ	-125.69	412816.10	-14898.10	-52398.20	518.74
ω	6.61	-14898.10	660.60	2209.32	-22.89
α	33.98	-52398.20	2209.32	27290.24	-131.67
$\log\phi$	-0.41	518.74	-22.89	-131.67	2.35